Power, Energy and Electrical Engineering
M. Deng (Ed.)

doi:10.3233/ATDE240304

Optimal Leveling Operation Scheduling of Microgrid for Distribution System Operator Using Virtual Power Interchange

Tomohiro KATSUZAKI [a,1], Ryuto SHIGENOBU [a], Akiko TAKAHASHI [a], Masakazu ITO [a], Norikazu KANAO [b], and Hitoshi SUGIMOTO [b]
[a] *Power System Laboratory, University of Fukui, Japan*
[b] *Innovation Laboratory, Hokuriku Electric Power Company, Japan*

Abstract. This study focuses on the development of an energy management system (EMS) for a microgrid (MG) that prioritizes balanced demand-supply operation to accommodate the stakes of distribution system operator (DSO), consumers (CNSs), and aggregator (AGR). An innovative EMS model for MG is introduced, which integrates power interchange (PIC) through electric vehicle aggregation tracks (EVATs) within virtual distribution feeders (VFs). This model enables each PIC to determine its contribution to different areas and corresponding remuneration simultaneously. The research presents a problem formulation for leveling operations using mixed integer linear programming (MILP), explaining operation scheduling through case studies. The results demonstrate the economic disadvantages for CNSs and AGR of completely leveling of net load powers by DSO's directives. Additionally, it is emphasized the significant role of PIC through EVATs, particularly in microgrids with surplus power of photovoltaic (PV) systems and less capacity of battery energy storage systems (BESSs).

Keywords. battery energy storage system (BESS), aggregation, energy management system (EMS), distribution system, mixed integer linear programming (MILP).

1. Introduction

Until recently, microgrids (MGs), which are small-scale energy management systems (EMSs), have attracted attention from the perspective of local production/consumption of energy, and various studies have been conducted [1]-[3]. Distributed power sources such as photovoltaic (PV) systems are used in MGs, and demand-supply coordination equipment such as battery energy storage systems (BESSs) are used to effectively utilize such energy. Recently, players such as aggregators (AGRs) in addition to distribution system operators (DSOs) and consumers (CNSs) have emerged, and it is important to schedule demand-supply operations while confirming the stakes of the three parties.

In addition, differences in the installation of PV systems and BESSs create differences in surplus power between areas. In order to solve this areal disparity, power interchange (PIC) using electric vehicles (EVs) has been devised [4]-[6]. An example of this could be peer-to-peer PIC between CNSs. In this case, it is difficult for DSO and

[1] Corresponding Author, Tomohiro Katsuzaki, Power System Laboratory, University of Fukui, 3-9-1, Bunkyo, Fukui 910-8507, Japan; E-mail: katsuzaki.tomohiro@pws.fuee.u-fukui.ac.jp.

AGR to grasp the contribution of PIC, making grid operation difficult. When AGR intervenes in PIC, it is necessary to simultaneously grasp both the contribution of the PIC to its own area and to other areas and to return these contributions to each area as rewards.

This study proposes an EMS model for MG that considers a PIC system (PICS) with virtual distribution feeders (VFs). Here, PICS with VFs is represented as an operation of EV aggregation tracks (EVATs). With the proposed PICS, it is possible to simultaneously determine the amount each PIC contributes to its own area and other areas, and the amount of remuneration to the area according to that contribution amount. Furthermore, we present a formulation of a mixed integer linear programming (MILP) problem for power flow leveling using the model and give examples of operation scheduling with them.

2. Energy Management System (EMS) Model for Microgrid (MG)

Figure 1 shows the schematics of the EMS model for MG. The EMS model consists of distribution feeders (DFs) in several areas. Each areal DF power flow consists of power flow from loads, PV system, BESS, and PICS. The loads consist of general loads (GLs) and EV charging loads, the PV system consists of panels and inverters, the BESS consists of inverters and batteries, and the PICS consists of VFs. The DF can consider electricity

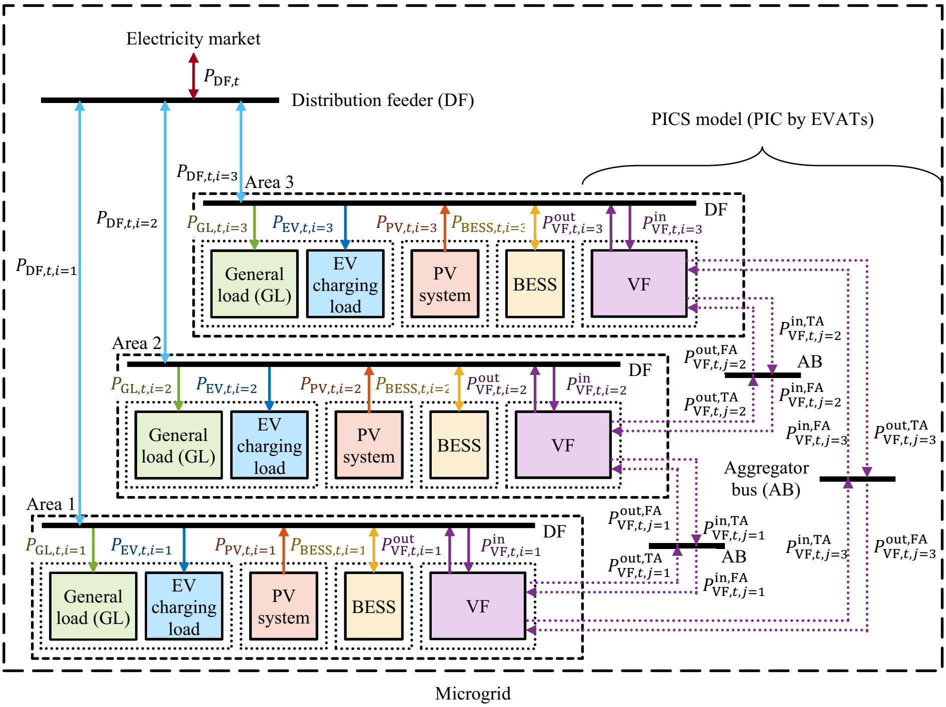

Figure 1. Schematic of energy management system (EMS) model for microgrid (MG) (three areas)

cost (basic cost and energy amount trade cost) and load leveling; the GL can consider locality, seasonality, weekdays, and holidays; the PV system can consider overloading and output control; the BESS can consider charge/discharge efficiency; the PICS can consider the operation of EVATs. Right side in Figure 1 shows a diagram of AGR's intervention in PIC between areas. The contribution of each PIC to its own area is expressed as $P_{\mathrm{VF},t,i}^{\mathrm{out}}$ and $P_{\mathrm{VF},t,i}^{\mathrm{in}}$ and the contribution to other areas is expressed as $P_{\mathrm{VF},t,j}^{\mathrm{out,TA}}$, $P_{\mathrm{VF},t,j}^{\mathrm{out,FA}}$, $P_{\mathrm{VF},t,j}^{\mathrm{in,TA}}$, and $P_{\mathrm{VF},t,j}^{\mathrm{in,FA}}$, where, t and i are index for time and area, respectively. These are determined simultaneously through optimization. $P_{\mathrm{GL},t,i}$ (power consumption of the GL), $P_{\mathrm{EV},t,i}$ (charging power of the EV load), and $P_{\mathrm{PV},t,i}^{\mathrm{gen}}$ (power generated by the PV system) are calculated from the model in [7], the model in [8], and the model in [9], respectively.

3. Formulation for Mixed Integer Linear Programming (MILP) Problem

In this paper, we use the formulation in [10] for constraints except for PICS. The remaining formulation is formulated as follows.

3.1. Objective Function for Distribution System Operator (DSO)

An objective function is formulated as follows to level each DF power flow,

$$\min\left(\sum_{t\in\mathcal{T}}\left(P_{\mathrm{DF},t}^{\mathrm{LE}}+\sum_{i\in\mathcal{I}}\left(P_{\mathrm{DF},t,i}^{\mathrm{LE}}\right)\right)+\omega\left(P_{\mathrm{DF}}^{\mathrm{abs,max}}+\sum_{i\in\mathcal{I}}\left(P_{\mathrm{DF},i}^{\mathrm{abs,max}}\right)\right)\right), \tag{1}$$

where, $\mathcal{T}$ and $\mathcal{I}$ are set of t and i, respectively, $P_{\mathrm{DF},t}^{\mathrm{LE}}$, $P_{\mathrm{DF},t,i}^{\mathrm{LE}}$ are leveling error (LE) of DF power flow [kW], $P_{\mathrm{DF}}^{\mathrm{abs,max}}$, $P_{\mathrm{DF},i}^{\mathrm{abs,max}}$ are absolute maximum power of DF power flow [kW], ω is weight.

The first term in Eq. (1) is the sum of the LEs of each DF, and the second term is the penalty term to optimize the DF maximum usage capacity for the calculation of the basic cost.

3.2. Constraints of Power Interchange System (PICS)

The constraints of PICS are formulated as follows. Here is an example of the case of three areas. PICS disaggregation is determined through optimization by expressing the power and cost or profit that VF contributes to DF in its own area and other areas using the constraints below,

$$0 \le P_{\mathrm{VF},t,i}^{d},\ \forall t\in\mathcal{T},\forall i\in\mathcal{I},\forall d\in\mathcal{D}, \tag{2}$$

$$0 \le P_{\mathrm{VF},t,j}^{v_1,v_2} \le C_{\mathrm{VF},t,j}^{v_3,\mathrm{TA}},\ \forall t\in\mathcal{T},\forall j\in\mathcal{J},\forall \boldsymbol{v}\in\mathcal{V}, \tag{3}$$

$$P_{\mathrm{VF},t,i} = P_{\mathrm{VF},t,i}^{\mathrm{out}} - P_{\mathrm{VF},t,i}^{\mathrm{in}},\ \forall t\in\mathcal{T},\forall i\in\mathcal{I}, \tag{4}$$

$$P^{d,h_2}_{\mathrm{VF},t,h_1} \le \begin{cases} C^{h_3,h_2}_{\mathrm{VF},t,h_1}\left(1 - b_{\mathrm{VF},t,h_1}\right) & (d = \mathrm{out}) \\ C^{h_3,h_2}_{\mathrm{VF},t,h_1} b_{\mathrm{VF},t,h_1} & (d = \mathrm{in}) \end{cases}, \quad , \qquad (5)$$
$$\forall t \in \mathcal{T}, \forall i \in \mathcal{I}, \forall j \in \mathcal{J}, \forall d \in \mathcal{D}, \boldsymbol{h} \in \mathcal{H}$$

$$P_{\mathrm{VF},t,i} = \begin{cases} \left. \begin{matrix} -P^{\mathrm{out,TA}}_{\mathrm{VF},t,j=1} + P^{\mathrm{in,FA}}_{\mathrm{VF},t,j=1} \\ -P^{\mathrm{in,TA}}_{\mathrm{VF},t,j=3} + P^{\mathrm{out,FA}}_{\mathrm{VF},t,j=3} \end{matrix} \right\} & (i = 1) \\ \left. \begin{matrix} -P^{\mathrm{out,TA}}_{\mathrm{VF},t,j=2} + P^{\mathrm{in,FA}}_{\mathrm{VF},t,j=2} \\ -P^{\mathrm{in,TA}}_{\mathrm{VF},t,j=1} + P^{\mathrm{out,FA}}_{\mathrm{VF},t,j=1} \end{matrix} \right\} & (i = 2) \\ \left. \begin{matrix} -P^{\mathrm{out,TA}}_{\mathrm{VF},t,j=3} + P^{\mathrm{in,FA}}_{\mathrm{VF},t,j=3} \\ -P^{\mathrm{in,TA}}_{\mathrm{VF},t,j=2} + P^{\mathrm{out,FA}}_{\mathrm{VF},t,j=2} \end{matrix} \right\} & (i = 3) \end{cases}, \ \forall t \in \mathcal{T}, \forall i \in \mathcal{I}, \qquad (6)$$

$$P^{d,\mathrm{FA}}_{\mathrm{VF},t,j} = \eta^{d}_{\mathrm{VF},j} P^{d,\mathrm{TA}}_{\mathrm{VF},t,j}, \ \forall t \in \mathcal{T}, \forall j \in \mathcal{J}, \forall d \in \mathcal{D}, \qquad (7)$$

$$Y^{\mathrm{AP}}_{\mathrm{VF},i} = \begin{cases} \left. \begin{matrix} +Y^{\mathrm{AC,out,TA}}_{\mathrm{VF},j=1} - Y^{\mathrm{AC,in,FA}}_{\mathrm{VF},j=1} \\ +Y^{\mathrm{AC,in,TA}}_{\mathrm{VF},j=3} - Y^{\mathrm{AC,out,FA}}_{\mathrm{VF},j=3} \end{matrix} \right\} & (i = 1) \\ \left. \begin{matrix} +Y^{\mathrm{AC,out,TA}}_{\mathrm{VF},j=2} - Y^{\mathrm{AC,in,FA}}_{\mathrm{VF},j=2} \\ +Y^{\mathrm{AC,in,TA}}_{\mathrm{VF},j=1} - Y^{\mathrm{AC,out,FA}}_{\mathrm{VF},j=1} \end{matrix} \right\} & (i = 2) \\ \left. \begin{matrix} +Y^{\mathrm{AC,out,TA}}_{\mathrm{VF},j=3} - Y^{\mathrm{AC,in,FA}}_{\mathrm{VF},j=3} \\ +Y^{\mathrm{AC,in,TA}}_{\mathrm{VF},j=2} - Y^{\mathrm{AC,out,FA}}_{\mathrm{VF},j=2} \end{matrix} \right\} & (i = 3) \end{cases}, \ \forall i \in \mathcal{I}, \qquad (8)$$

$$Y^{\mathrm{AC},d,p}_{\mathrm{VF},j} = \sum_{t \in \mathcal{T}} \left(y^{\mathrm{AC},p}_{\mathrm{VF},t,j} P^{d,p}_{\mathrm{VF},t,j} \Delta t \right), \ \forall j \in \mathcal{J}, \forall d \in \mathcal{D}, \forall p \in \mathcal{P}, \qquad (9)$$

$$Y^{\mathrm{AP}}_{\mathrm{VF}} = \sum_{j \in \mathcal{J}} \left(Y^{\mathrm{AC,out,FA}}_{\mathrm{VF},j} - Y^{\mathrm{AC,out,TA}}_{\mathrm{VF},j} + Y^{\mathrm{AC,in,FA}}_{\mathrm{VF},j} - Y^{\mathrm{AC,in,TA}}_{\mathrm{VF},j} \right), \qquad (10)$$

where, j, d, p, $\boldsymbol{v} = [v_1 \quad v_2 \quad v_3]$, and $\boldsymbol{h} = [h_1 \quad h_2 \quad h_3]$ are index for PIC route, PIC direction for out/in, PIC path for to/from AGR, capacity constraints of PIC, and PIC with exclusivity, respectively, $\mathcal{J}$, $\mathcal{D} = \{\mathrm{out}, \mathrm{in}\}$, $\mathcal{P} = \{\mathrm{TA}, \mathrm{FA}\}$, $\mathcal{V} = \{[\mathrm{out} \quad \mathrm{TA} \quad \mathrm{out}], [\mathrm{out} \quad \mathrm{FA} \quad \mathrm{in}], [\mathrm{in} \quad \mathrm{TA} \quad \mathrm{in}], [\mathrm{in} \quad \mathrm{FA} \quad \mathrm{out}]\}$, and $\mathcal{H} = \{[i \quad \emptyset \quad \emptyset], [j \quad \mathrm{TA} \quad d]\}$ are set of j, d, p, $\boldsymbol{v}$, and $\boldsymbol{h}$, respectively, $\emptyset$ is empty of index (ex. $C^{\emptyset,\emptyset}_{\mathrm{VF},t,i} = C_{\mathrm{VF},t,i}$), $P_{\mathrm{VF},t,i}$, $P^{d}_{\mathrm{VF},t,i}$, and $P^{d,p}_{\mathrm{VF},t,j}$ are VF power flow [kW], $C_{\mathrm{VF},t,i}$ and $C^{d,\mathrm{TA}}_{\mathrm{VF},t,j}$ are capacity of VF [kW], $b_{\mathrm{VF},t,i}$ and $b_{\mathrm{VF},t,j}$ are state of direction of VF power flow, $\eta^{d}_{\mathrm{VF},j}$ is efficiency of PIC, $y^{\mathrm{AC},p}_{\mathrm{VF},t,j}$ is unit price of PIC [JPY/kWh], Δt is time granularity [hour], $Y^{\mathrm{AC},d,p}_{\mathrm{VF},j}$ is daily total energy amount trade cost of $P^{d,p}_{\mathrm{VF},t,j}$ [JPY], $Y^{\mathrm{AP}}_{\mathrm{VF},i}$ is daily total energy amount trade profit of CNS [JPY], $Y^{\mathrm{AP}}_{\mathrm{VF}}$ is daily total energy amount trade profit of AGR [JPY].

Eq. (2) and (3) show various upper and lower limit constraints. Eq. (3) to (5) show exclusive constraints on outflow/inflow. Eq. (4) to (7) show constraints regarding VF power flow. Eq. (8) to (10) show constraints regarding the cost or profit of PIC. Eq. (4) is an equality constraint that shows the decomposition of outflow/inflow power flow into outflow power flow and inflow power flow. Eq. (5) ensures exclusivity of PIC. Eq. (6)

shows the power flow that PICS with VFs contributes to the DF in its own area. Eq. (7) shows the efficiency of PIC between areas, and as $\eta^{d}_{\mathrm{VF},j} < 1$ when it is considered as PIC by EVATs ($\eta^{d}_{\mathrm{VF},j}$ takes into account the running, charging, and discharging losses of EVATs). Eq. (8) records the contribution as CNS's trading profit. Eq. (9) accounts for the contribution of PIC to DF in other areas as a transaction cost. Eq. (10) shows the total trading profit of AGR by PICS.

3.3. Constraints of Stakes of Players

The constraints of the stakes of players are formulated as follows,

$$Y^{\mathrm{TC}}_{\mathrm{DF},i} \leq Y^{\mathrm{TC,bef}}_{\mathrm{DF},i}, \ \forall i \in \mathcal{I}, \tag{11}$$

$$Y^{\mathrm{AP,bef}}_{\mathrm{DF}} + Y^{\mathrm{AP,bef}}_{\mathrm{VF}} \leq Y^{\mathrm{AP}}_{\mathrm{DF}} + Y^{\mathrm{AP}}_{\mathrm{VF}}, \tag{12}$$

where, $Y^{\mathrm{TC}}_{\mathrm{DF},i}$ and $Y^{\mathrm{TC,bef}}_{\mathrm{DF},i}$ are daily total electricity cost of CNS after and before optimization [JPY], respectively, $Y^{\mathrm{AP}}_{\mathrm{DF}}$, $Y^{\mathrm{AP,bef}}_{\mathrm{DF}}$, $Y^{\mathrm{AP}}_{\mathrm{VF}}$, and $Y^{\mathrm{AP,bef}}_{\mathrm{VF}}$ are daily total energy amount trade profit of AGR after and before optimization at DF and VF [JPY], respectively.

Eq. (11) indicates that the total cost of the CNS should not become larger than before optimization. Eq. (12) constrains the AGR profit from decreasing compared to before optimization.

Here, in Eq. (1) to (12), $P^{\mathrm{LE}}_{\mathrm{DF},t}$, $P^{\mathrm{LE}}_{\mathrm{DF},t,i}$, $P^{\mathrm{abs,max}}_{\mathrm{DF}}$, $P^{\mathrm{abs,max}}_{\mathrm{DF},i}$, $P_{\mathrm{VF},t,i}$, $P^{d}_{\mathrm{VF},t,i}$, $P^{d,p}_{\mathrm{VF},t,j}$, $b_{\mathrm{VF},t,i}$, $b_{\mathrm{VF},t,j}$, $Y^{\mathrm{AC},d,p}_{\mathrm{VF},j}$, $Y^{\mathrm{AP}}_{\mathrm{VF},i}$, $Y^{\mathrm{TC}}_{\mathrm{DF},i}$, $Y^{\mathrm{AP}}_{\mathrm{DF}}$, and $Y^{\mathrm{AP}}_{\mathrm{VF}}$ are decision variables, and the other variables are parameters.

4. Case Study

4.1. Simulation Conditions

EMS operations are scheduled using three cases as examples. Case 0 shows before optimization, Case 1 considers the Constraints of the stakes of players, Case 2 does not.

Simulation conditions for common to all cases are shown in Table 1. In all cases, the simulation period is one day on a weekday in May, which has the most sunshine of the average year in Imajo's three areas (residential area, commercial area, industrial area), Fukui, Japan. It is assumed that the PV panels will be installed facing south at an angle of 30 degrees. The unit price of transactions between AGR and the electricity market is selected from [11] as a time-varying unit price. Figure 2 shows the power consumption of the GL calculated from the model in [7], Figure 3 shows the charging power of the EV load calculated from the model in [8], and Figure 4 shows the power generated by the PV system calculated from the model in [9].

Table 1. Simulation conditions common to all cases

Exogenous variables				
Item	**Unit**	**Value**		
		Residential $i = 1$	Commercial $i = 2$	Industrial $i = 3$
PV inverter capacity	kW	4,000	800	800
PV panel capacity	kW	4,000	800	800
BESS inverter capacity	kW	3,000	240	240
BESS battery capacity	kWh	12,000	960	960

Item	**Unit**	**Value**
Time granularity	hour	0.5
DF capacity	kW	5,500
Daily unit price of basic cost of CNS	JPY/kW	10
Unit price of energy amount trade cost of CNS (purchase from AGR)	JPY/kWh	32
Unit price of energy amount trade cost of CNS (sell to AGR)	JPY/kWh	8
Efficiency of charge/discharge of BESS	-	0.95
Upper limit of state of charge (SOC) of BESS	-	0.8
Lower limit of SOC of BESS	-	0.2
Efficiency of PIC	-	0.85
Unit price of PIC from CNS to AGR	JPY/kWh	16
Unit price of PIC from AGR to CNS	JPY/kWh	24
Weight	-	0.00001

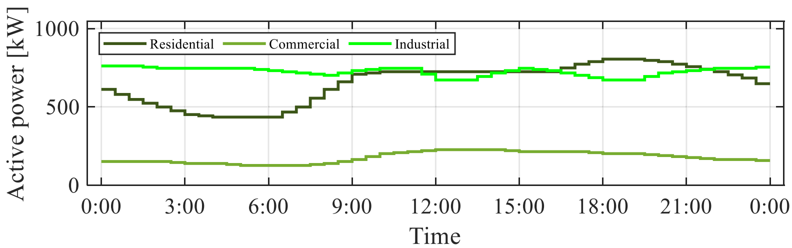

Figure 2. Power consumption of general load (GL)

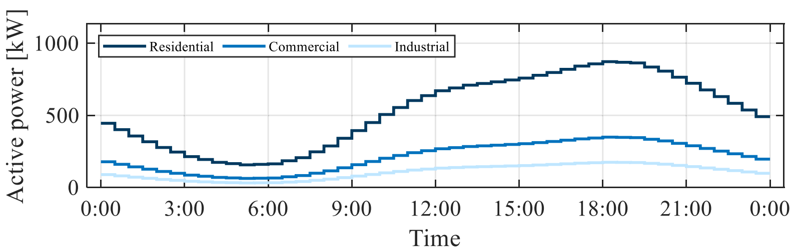

Figure 3. Charging power of electric vehicle (EV) load

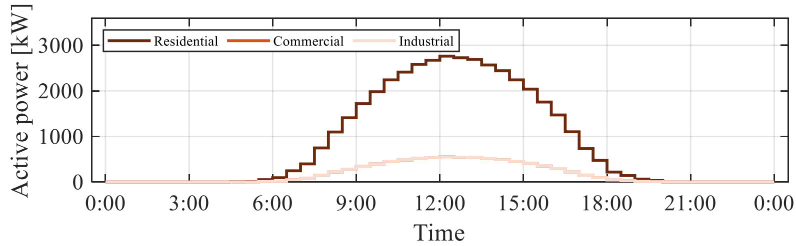

Figure 4. Power generated by photovoltaic (PV) system

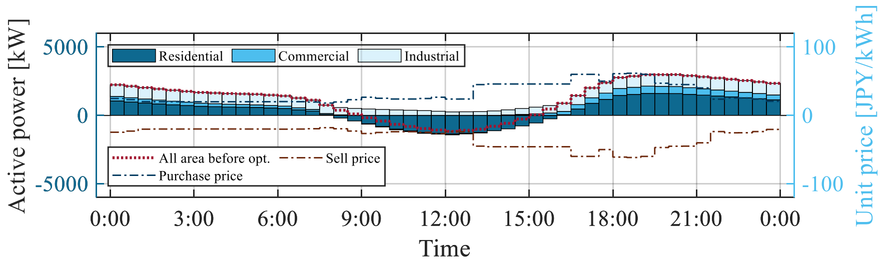

Figure 5. Distribution feeder (DF) power flow before optimization (Case 0)

Figure 5 shows the DF power flow in case 0. Here, the sell price and the purchase price in the figure indicate the unit price of transactions between AGR and the market. From Figure 5, it can be seen that there is a mixture of areas where surplus power is generated from 8:00 to 16:00 and areas where it is not in Case 0.

4.2. Simulation Results

Table 2 and Figure 6 show simulation results regarding costs and the derived optimal operation scheduling for each case, respectively. For each graph in Figure 6, from top to bottom, the power flow of DF, BESS power, power contributed to the own area by PICS, PV suppression power, state of charge (SOC) of BESS, and power contributed to other areas by PICS are shown. In the power flow of DF, the blue bar graph shows power bought/sold by CNS from/to AGR (positive: power purchased from AGR), and the dark red step graph shows power bought/sold by AGR from/to the market (positive: power purchased from the market). Positive in BESS power indicates discharge, positive in power contributed by PICS to its own area is an outflow (equivalent to selling electricity from CNS to AGR), and positive in power contributed to other areas by PICS indicates forward direction as described in the legend. Here, the power contributed to other areas by PICS is the disaggregated power contributed to the own area.

Table 2. Simulation results regarding costs

Case	Consumer (CNS)							
	Purchases from AGR [JPY]				Sales to AGR [JPY]			
	Res.	Com.	Ind.	All area	Res.	Com.	Ind.	All area
0	479,687	173,468	506,607	1,159,762	57,462	1,610	0	59,072
1	449,386	160,480	482,284	1,092,150	597	0	0	597
2	467,272	236,471	590,373	1,294,116	0	0	0	0

Case	CNS							
	Basic cost (contract fee to DSO) [JPY]				PIC profit [JPY]			
	Res.	Com.	Ind.	All area	Res.	Com.	Ind.	All area
0	16,057	5,342	8,775	30,174	0	0	0	0
1	8,013	3,969	8,627	20,609	18,519	-12,751	-24,470	-18,702
2	6,084	3,079	7,687	16,850	-13,437	-5,767	7,582	-11,622

Case	CNS							
	Total cost [JPY]				PV output curtailed amount [kWh]			
	Res.	Com.	Ind.	All area	Res.	Com.	Ind.	All area
0	438,282	177,200	515,381	1,130,864	0	0	0	0
1	438,282	177,200	515,381	1,130,864	3,696	0	0	3,696
2	486,793	245,317	590,478	1,322,588	6,311	2,134	1,865	10,310

Case	Aggregator (AGR)								
	Trades at market [JPY]		PIC profit [JPY]						Total profit [JPY]
	Purchases	Sales	Res. to Com.	Com. to Res.	Com. to Ind.	Ind. to Com.	Ind. to Res.	Res. to Ind.	
0	1,140,253	138,596	0	0	0	0	0	0	99,032
1	1,011,223	0	5,520	3,183	348	0	2,645	7,004	99,032
2	1,293,240	0	2,508	2,185	686	988	3,811	1,443	12,498

Case	Distribution system operator (DSO)							
	Cumulative absolute leveled error [kW]				DF maximum usage capacity [kW]			
	Res.	Com.	Ind.	All area	Res.	Com.	Ind.	All area
0	40,263	7,783	8,690	56,234	1,606	534	877	2,984
1	4,089	2,725	6,313	13,127	801	397	863	2,061
2	0	0	0	0	608	308	769	1,685

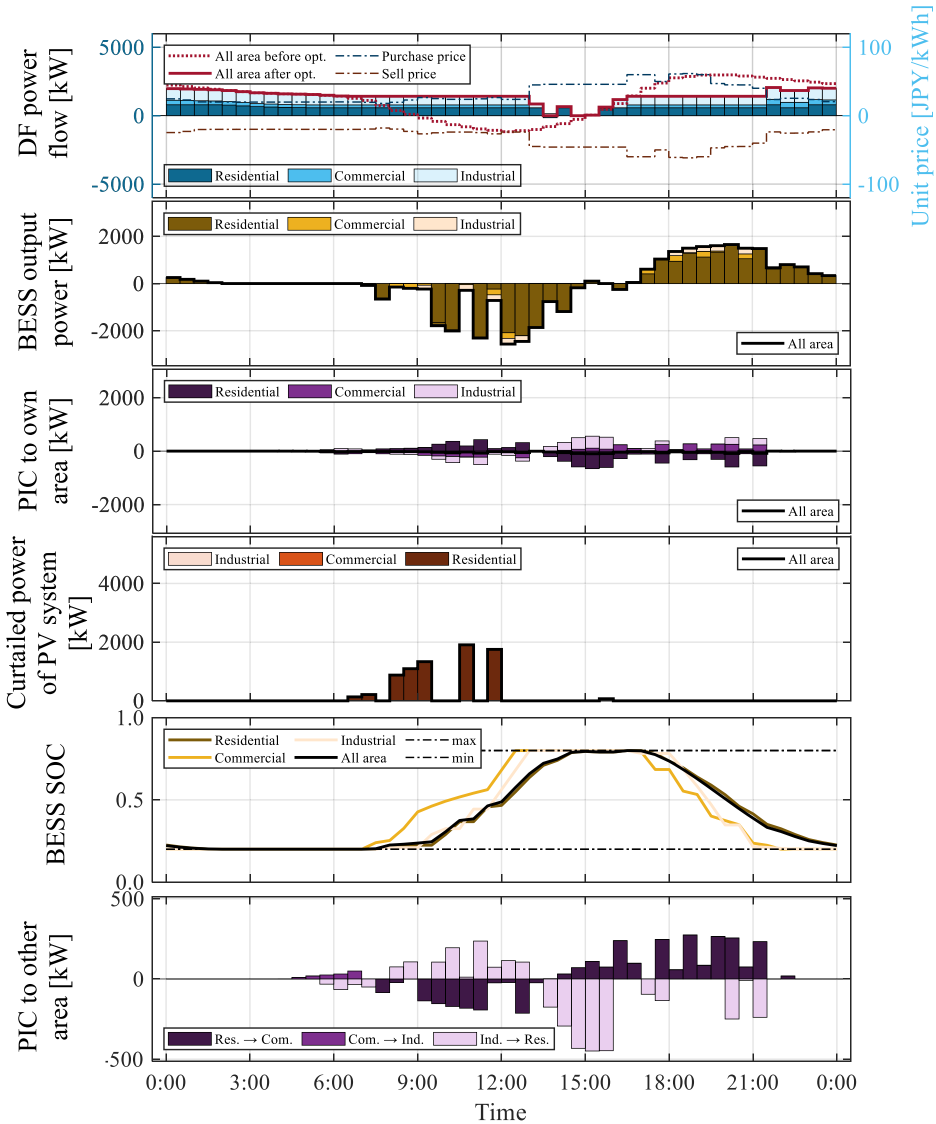

(a) Case 1 (power flow leveling **with** constraints of stakes of players)

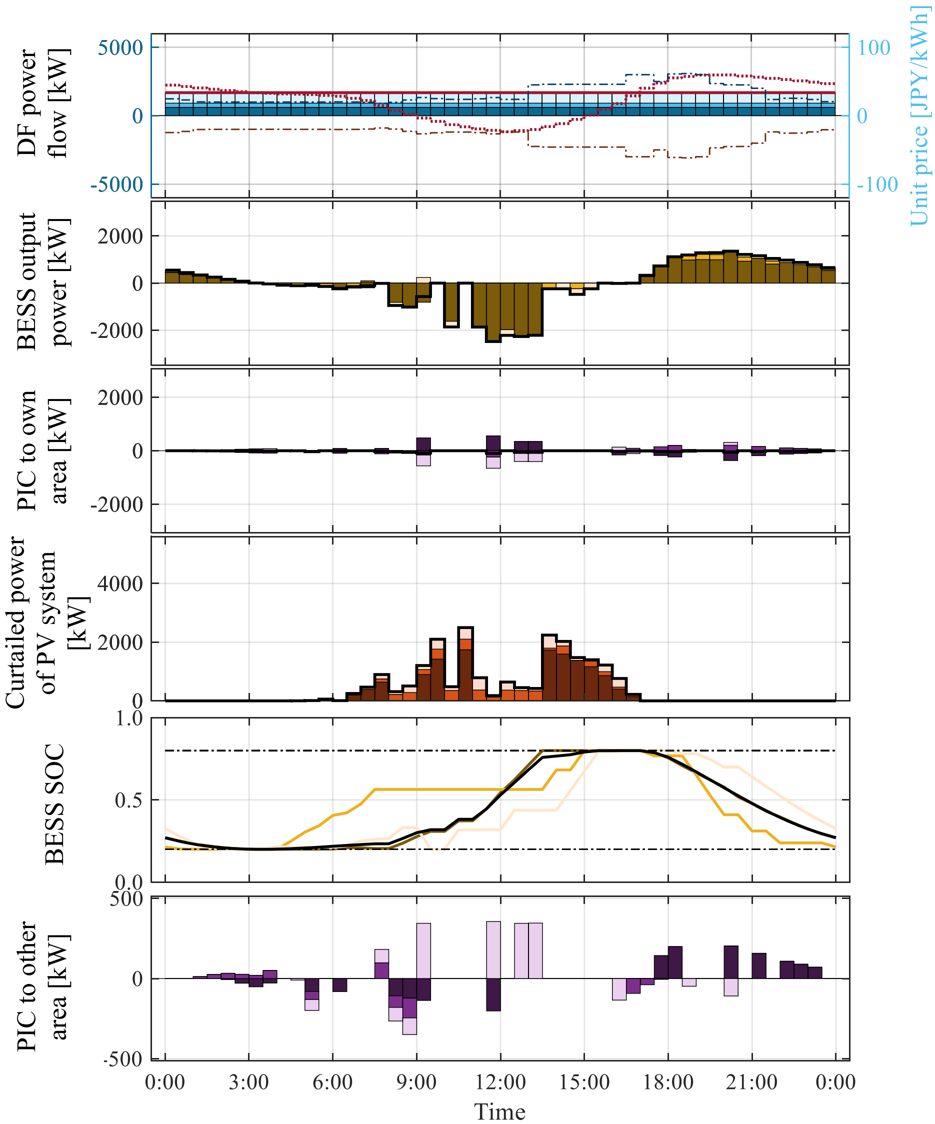

(b) Case 2 (power flow leveling **without** constraints of stakes of players)

Figure 6. Optimal operation scheduling of microgrid (MG) for each case

The cumulative absolute leveling error values in the blue fill of Table 2 are 4,089 kW, 2,725 kW, and 6,313 kW for Case 1, which are not 0 kW in any area, confirming that complete leveling has not been achieved. On the other hand, Case 2 has 0 kW in any of the areas, thus perfect leveling has been achieved. From the DF power flow after optimization in Figure 6 (a), it can be seen that in Case 1, leveling is not achieved between 13:00 and 16:30. In order to achieve leveling, it is necessary to increase the power purchased from the grid by charging the BESS or by curtailing the PV power. During this time period, the SOC has reached its upper limit and charging is not possible.

In addition, increasing PV output suppression is undesirable because PV surplus power leads to lower electricity prices for the CNS and higher profits for AGR. From the range enclosed by the blue box in Table 2, Case 0 and Case 1 show the same values and any further PV output suppression would violate the constraints in Eq. (11) and (12). Therefore, it can be seen that the curtailed power is almost zero during this time period in Figure 6 (a). On the other hand, since the constraints Eq. (11) and (12) are not considered in Case 2, the PV output curtailment increases in Figure 6 (b), indicating that perfect leveling is achieved. At this time, from the blue box in Table 2, it can be seen that the cost of CNS increases and the profit of AGR decreases in Case 2 compared to Case 0 and Case 1. From the above, it can be seen that in these cases, it is economically disadvantageous to the CNS and AGR for the DSO to order complete leveling, and the operation schedule that maximizes leveling without causing economic disadvantage to the CNS and AGR is given as Case 1.

In the case of leveling, the sales amount of CNS and AGR decreases, as shown in the purple box in Table 2. This leads to an increase in the cost of CNS and a decrease in the profit of AGR. Therefore, it can be seen that Case 1, which takes into account the constraints in Eq. (11) and (12), plans to earn more electricity sales from the PICs, as indicated by the purple fill. In particular, Figure 6 (a) shows that PIC to other areas is performed from other areas to the residential area from 7:30 to 13:30, and from a residential area to other areas from 13:30 to 22:30. In addition, the SOC of the BESS shows that the SOCs of the non-residential areas reach the upper limit earlier during charging and the SOCs reach the lower limit earlier during discharging than that of the residential area. These indicate that the battery capacity to handle surplus power for leveled operation has a margin in the residential area, but not in the other areas. Therefore, it can be assumed that PICs are being transferred from other areas to the residential area from 7:30 to 13:30 and from the residential area to other areas from 13:30 to 22:30 to compensate for the lack of charge/discharge of the BESS. These PICs also increase in Case 1, which considers constraints Eq. (11) and (12). In summary, we found that PICs by EVATs are actively performed in microgrids with areal disparities in surplus power and BESS capacity when load leveling operations are performed considering CNS and AGR stakes.

5. Conclusion

In the EMS of MG, which has become extremely diversified in recent years, it is important to establish a schedule for supply and demand operations while confirming the interests of the three parties (DSO, CNS, and AGR). Inter-CNS PIC via AGR is effective in eliminating disparities in surplus electricity between areas. In this study, we proposed the EMS model for MG considering PIC by EVATs as PICS with VFs. In the proposed PICS, it is possible for each PIC to simultaneously determine the amount of contribution to its own area and other areas, and the amount of remuneration to the area according to the amount of contribution. Furthermore, we presented the formulation of the MILP problem that enables leveling operation and demonstrated examples of operational scheduling using them. As the result, we were able to obtain that it is economically disadvantageous to the CNS and AGR for the DSO to order complete leveling. Also, we were able to find that PICs by EVATs are actively performed in microgrids with areal disparities in surplus power and BESS capacity when load leveling operations are performed considering CNS and AGR stakes. In the future, we plan to consider the objective functions on the CNS and AGR sides and compare the results.

Acknowledgements

This work was supported by Hokuriku Electric Power Company and the Graduate Program for Power Energy Professionals, Waseda University from MEXT WISE Program.

References

[1] Luo L, Abdulkareem SS, Rezvani A, Miveh MR, Samad S, Aljojo N, et al. Optimal scheduling of a renewable based microgrid considering photovoltaic system and battery energy storage under uncertainty. J Energy Storage. 2020 Apr;28:101306.
[2] Jiang W, Wang XH, Huang HY, Zhang DL, Ghadimi N. Optimal economic scheduling of microgrids considering renewable energy sources based on energy hub model using demand response and improved water wave optimization algorithm. J Energy Storage. 2022 Nov;55:105311.
[3] Duan YZ, Zhao YY, Hu JP. An initialization-free distributed algorithm for dynamic economic dispatch problems in microgrid: Modeling, optimization and analysis. Sustainable Energy Grids & Networks. 2023 Jun;34:101004.
[4] Ravi SS, Aziz M. Utilization of Electric Vehicles for Vehicle-to-Grid Services: Progress and Perspectives. Energies. 2022 Jan;15(2):589.
[5] Ahmadi SE, Marzband M, Ikpehai A, Abusorrah A. Optimal stochastic scheduling of plug-in electric vehicles as mobile energy storage systems for resilience enhancement of multi-agent multi-energy networked microgrids. J Energy Storage. 2022 Nov;55:105566.
[6] Li Y, Hara R, Kita H. Management and economic merits of wide-area cooperation among microgrids coupled with MaaS. IEEJ Trans PE. 2022 Nov;142(11):552-560.
[7] Model III: 66 kV Suburban system model [Internet]. Tokyo (Japan): IEEJ. 1999 - [updated 2001 Sep 19; cited 2023 Oct 13]. Available from: http://www2.iee.or.jp/~pes/model/english/index.html.
[8] Oda T, Ito M, Kawasaki N, Miyazaki T, Kashiwagi T. Potential estimation of hourly blank storage space and charge loads of EVs using road traffic census and vehicles status. IEEJ Trans PE. 2011 Dec;131(12): 920-926.
[9] AES Center, Tokyo Institute of Technology. Medium-scale/large-scale solar power generation system. Tokyo: Ohmsha; 2016. p. 82-83.
[10] Katsuzaki T, Shigenobu R, Ito M. Optimization problem of local power supply and demand by cross-regional power-interchange for diversified aggregation businesses. 2023 IEEJ Joint Tech Meeting Rec on PE PSE SPC. 2023 Mar;3: 57-63.
[11] Market data [Internet]. Tokyo (Japan): Japan Electric Power Exchange. 2017 May - [cited 2023 Oct 13]. Available from: https://www.jepx.jp/nonfossil/market-data/.